IEEE Sensors Letters Volume 2(3) (2017)
IEEE Sensors Council
Article Subject (see Index Terms below and write one here) ____________________

Methodological Framework for Conductor Lifetime Estimation Using Optical Sag Sensors

Himanshi Singh[1,2*], Grzegorz Fusiek[1**], and Pawel Niewczas[1**]
[1] Department of Electronic and Electrical Engineering, University of Strathclyde, Glasgow, UK
[2] National Physical Laboratory (NPL), Teddington, Middlesex, UK
* Student Member, IEEE
** Member, IEEE

Abstract—This letter proposes the methodological framework for estimating overhead line (OHL) conductor lifetime using optical sag sensors. The sensors utilize fiber Bragg grating (FBG) technology to monitor static and dynamic mechanical parameters of the conductor in real-time, including direct measurements of strain and temperature that can be translated into the sag, force, stress readings. The signals acquired by the sensors in a field trial were used to analyze vibration and dynamic stress load experienced by the monitored conductor to predict its cumulative damage by means of the rainflow counting algorithm combined with the Miner's rule. The results suggest that the proposed methodology allows for online estimation of the remaining lifetime of the conductor under dynamic operating conditions in ambient environments.

Index Terms— hard-drawn copper conductor, fiber Bragg gratings, fatigue life, sag sensor

I. INTRODUCTION

Environmentally induced fatigue of overhead line conductors deteriorates their structural integrity, negatively impacting on the long-term reliability of power delivery. Overhead lines (OHLs) play a vital role in the efficient and widespread delivery of electrical energy but are subjected to diverse environmental and operational stresses, such as wind loads, temperature changes and dynamic loads from line oscillations and ice accumulation, all of which lead to failures. The fatigue life of these conductors is assessed using variable amplitude testing designed to simulate real-world conditions. The estimated lifespan of a conductor hinges on the interplay among its material properties, design and applied loads. A common problem in overhead lines is fretting, caused by aeolian vibrations, where minimal relative movements at the contact points between conductors and other line components result in surface damage. Repeated stress application over time initiates and propagates cracks or other structural defects. Unlike static loads, the cyclic stresses unique to OHLs present special challenges in fatigue management. Addressing fatigue concerns is essential for the safety and reliability of power transmission.

Historically, real-time and experimental studies have documented fretting-induced failures in conductors [1]-[3]. Finite element modelling has been utilized to predict the lifetime of high-temperature low-sag (HTLS) conductor by homogenizing the conductor's geometry [4]. Solutions proposed [5] include increasing the voltage to reduce current and thus reducing sag. The aeolian vibration fatigue has been approached through the energy balance model (EBM). Introduced in the 1960s, the Everyday Tension concept (EDT) sought to cap conductor tension within safe design limits, a practice that has evolved over decades to include vibrational considerations within transmission lines [6-9].

Despite these measures, failures have persisted, prompting the introduction of a new safe tension limit based on practical assessments. The rainflow counting algorithm, initially developed for mechanical engineering, plays a crucial role in OHL fatigue analysis by effectively quantifying cyclic loading effects. When combined with the stress-life (S-N) curves of the materials and Miner's rule for the cumulative damage estimation it can provide estimates of the remaining lifetime of the material.

The paper proposes a methodology to predict lifetime of hard-drawn copper (HDC) conductor using sag sensor previously developed by the authors [10]-[13]. The outcomes of OHL sag and vibration measurements, taken by the sag sensors during a field trial at the Power Network Demonstration Centre (PNDC), University of Strathclyde, UK, are utilized to predict OHL durability. The highest vibration amplitude recorded by the sensor in the span is used to estimate the lifetime of the conductor using rainflow counting algorithm and Miner's rule for cumulative damage. The differentiating factor in the use of FBG-based OHL sensors as proposed in our manuscript is that they can be passively interrogated and multiplexed over extended distances. The information at the central sensor interrogator can be utilized by the power network operator to perform better informed decisions, for example implement improved dynamic line rating procedures. Moreover, such sensors are compatible with FBG-based current and voltage sensors and thus a holistic power grid condition monitoring and control system can be realized in a cost-effective fashion.

II. OPTICAL SAG SENSOR IN A FIELD TRIAL

A. Sensor Design and Construction

The proposed design and construction of the sag sensor was

Corresponding author: H. Singh (himanshi.singh@strath.ac.uk). Digital Object Identifier: 10.1109/LSEN.XXXX.XXXXXXX (inserted by IEEE).

previously presented by the authors in [10]. Briefly, a commercial bespoke version of the T220 strain sensor from Technica SA suitable for operation up to 200 ˚C was utilized together with customized sensor installation metallic structures to measure mechanical parameters of an OHL conductor. The sag sensor contains both strain and temperature measuring FBGs that are packaged in a stainless steel 316 (SS316) enclosure and equipped with 0.2 mm SS304 shims for spot welding onto the structure being monitored [10]-[12]. Since the T220 sensor cannot be directly mounted on the transmission lines, custom-made SS304 plates and clamps were designed to allow for installation of the sag sensor on a conductor to facilitate measurements of sag, temperature, and vibration at temperatures up to 200 ˚C. It was demonstrated by the force and temperature characterization and calibration that the sensor is suitable for monitoring standard low-temperature and HTLS line conductors [11]-[12].

B. Field Trial Setup

The first sag sensor prototypes with different mounting plates were designed for installation on a hard-drawn copper conductor, with a diameter of 10.5 mm and a cross-section of 70 mm^2 as such a conductor was available on an OHL at PNDC [10], [12]-[13]. The conductor instrumented with two sag sensors, had 7 strands with a strand diameter of 3.5 mm. The span length of the line measured with a distance meter was 88 m. At 10 ˚C, the tension force measured in the conductor with a dynamometer was 3.45 kN [13]. A photograph of two sag sensors (S1 and S2) installed on the HDC middle conductor of the line is shown in Fig.1. [13].

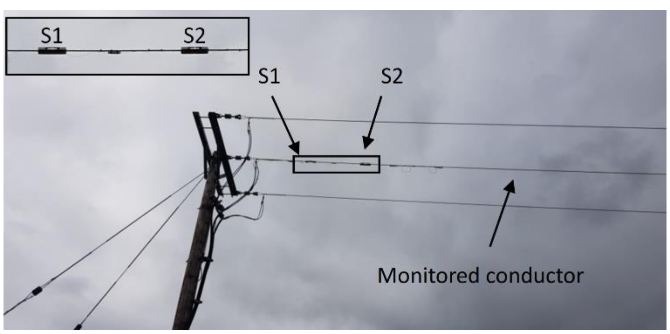

Fig. 1. Sag sensor installed on an OHL conductor at PNDC, University of Strathclyde, UK [13].

The two sag sensors were installed on the middle conductor of the line, approximately 2 meters from the pole, and about 1 meter apart from each other [13]. During the field trial, the sensors were interrogated with a dedicated FBG interrogator and the signals from the sensors were logged every 4 h for 1 min or occasionally longer, e.g., for 5 min continuously.

III. FATIGUE LIFE ESTIMATION METHODOLOGY

A. Rainflow Counting Algorithm

The rainflow counting algorithm, first proposed by Matuishi and Endo [14], uses a recursive approach to identify closed hysteresis loops in strain-stress plots, metaphorically described as the path of raindrops on a pagoda roof. Later, a non-recursive form of the algorithm was outlined [15], which is utilized in this paper. Rainflow counting is crucial for fatigue analysis as it identifies and counts stress cycles from a load signal, aiding in the assessment of material fatigue life under variable load conditions.

The principle of the rainflow counting algorithm is shown in Fig. 2 and its steps are as follows. Identifying a turning point in a stress signal where the direction changes, either from increasing to decreasing (peak) or from decreasing to increasing (valley). The time history signal is traversed to pinpoint these turning points. Pairs of turning points are connected to form closed loops, with each cycle the material undergoes. For each cycle, the range ($\Delta\sigma$) and mean (σ_{mean}) values are calculated. The range is the stress difference between the peak and the valley, while the mean is the cycle's average stress. Each unique range and mean pair are counted, and the counted cycles from the original signal are removed, leaving behind residuals for further analysis. The residuals are continued to be analyzed until all cycles are accounted for. The data is compiled into a matrix to represent the load history. Each row of the matrix corresponds to a different range-mean pair, with the elements of the matrix indicating the frequency of each pair [14].

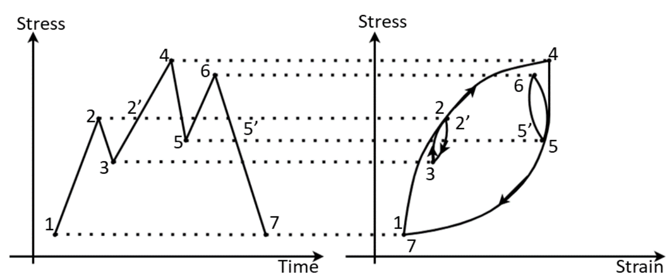

Fig. 2. Rainflow Counting Algorithm principle.

These cycles are then used in conjunction with fatigue analysis methods, such as the Palmgren-Miner rule, to estimate the fatigue life of the material under variable loading conditions.

B. S-N curves

The assessment of fatigue performance in materials is typically conducted using the stress-life method, which utilizes S-N curves (also known as Wöhler curves). These curves illustrate the relationship between cyclic stress amplitude (S) and the number of cycles until failure (N) observed during laboratory testing. The test is considered complete when either 10 % of the cable's wires have failed or a predetermined number of wires break. Due to the complex nature and high costs of conducting these tests, the International Council on Large Electric Systems (CIGRÉ) has introduced a standardized curve, known as the CIGRÉ Safe Border Line (CSBL), which helps companies estimate the lifespan of conductors without substantial financial outlays [13]. The following equation can define the Safe Border Line curve [16],

$$\sigma = A \cdot N_i^B \quad (1)$$

where, A and B are constants related to number of fatigue cycles N_i for a given stress level and the number of conductor layers, while σ represents the stress amplitude. The data is depicted as S-N curve, corresponding to each stress level to the correlating number of cycles.

The cumulative damage of the conductor can be estimated through the application of Miner's rule, utilizing the following expression [16] is:

$$D = \Sigma_{i=1}^{m} \frac{n_i}{N_i} \qquad (2)$$

where, n_i represents the number of cycles at stress level σ_i and N_i is the fatigue life at stress level σ_i. The D value equal or greater than 1 means the material failure due to fatigue.

The remaining lifetime of the sample under test can be calculated by using the equation:

$$V = \frac{1}{D} \qquad (3)$$

where, D is defined as the cumulative damage and V is the remaining life in cycles.

C. Conductor Lifetime Estimation Methodology

As can be seen in Fig. 1, the PNDC line conductors are fixed to the poles with non-ceramic strain insulators which are typically used at points where the conductor changes direction or where there is tension, such as at dead-ends or corners [13]. While strain insulators provide necessary support and help manage mechanical stresses, they may introduce some rigidity into the system compared to suspension insulators. The rigidity of strain insulators could potentially lead to localized stress concentrations at attachment points, which may affect conductor fatigue lifetime, especially in environments with significant temperature variations or dynamic loading conditions due to wind. Therefore, monitoring of mechanical parameters of conductors is of great importance and highly demanded.

As demonstrated in [13], the previously proposed optical sag sensors are capable of detecting a wide range of wind-induced vibration, including aeolian vibrations, galloping or wake-induced oscillations. Assuming that the line would experience such vibration for a long time, its fatigue life expectancy can be estimated using the equations presented in section IIIB.

An example of a 5-minute continuous record of vibration detected by the optical sag sensor S1 in the monitored HDC conductor at PNDC is shown in Fig 3. The wavelength changes in sensor S1 shown in Fig. 3 (a) were obtained by removing the mean component from the optical signal presented in [13]. Using the sensor characteristics and the conductor specifications [12], the maximum dynamic stress detected in the conductor during this measurement window was estimated to be approximately 10 MPa peak-to-peak, as shown in Fig. 3 (b). This stress range is over 3 times lower than the endurance level of HDC conductors (35 MPa) [17], indicating that the monitored conductor was operated in the endurance strength region of the material S-N curve, in these particular environmental conditions. Since the limited experimental field data did not capture sufficient vibration to effect damaging stresses to the conductor, the real stress signal was scaled up by a factor of 10 to allow for illustrating the principle of analysis that is proposed in this paper. Consequently, the stress range was increased to 116 MPa as depicted in Fig. 3 (c).

To predict the remaining lifetime of the monitored conductor, the scaled-up stress data was analyzed using the rainflow counting algorithm combined with the cumulative damage estimation. For the analysis, modified MATLAB rainflow counting functions based on the algorithms proposed in [18] were used.

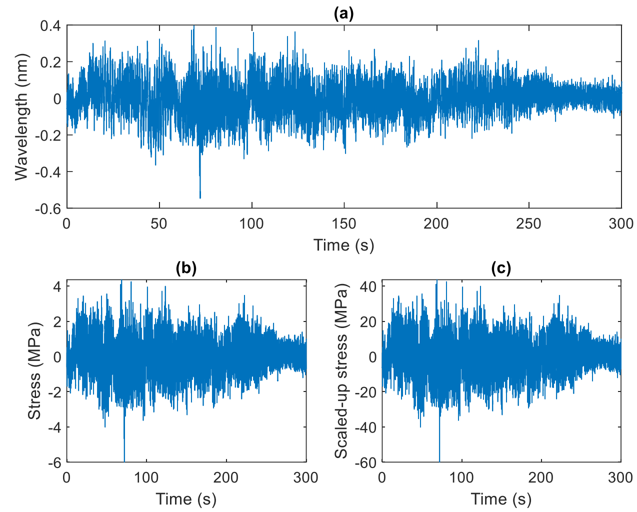

Fig. 3. Change in wavelength in sensor S1 monitoring the HDC conductor at PNDC [13] (a) converted to stress in the conductor (b) and stress scaled up for fatigue analysis purposes (c).

A 5-second window of the analyzed scaled-up stress signal is shown in Fig. 4 together with the stress turning points resulted from the rainflow filtering procedure discussed in section IIIA. The detection of the load reversal points can be adjusted by the stress threshold which in this case was set to 5% of the maximum detected stress range (116 MPa) [19]. Its settings help filtering out the stress levels which do not significantly contribute to the material fatigue and can be neglected [20].

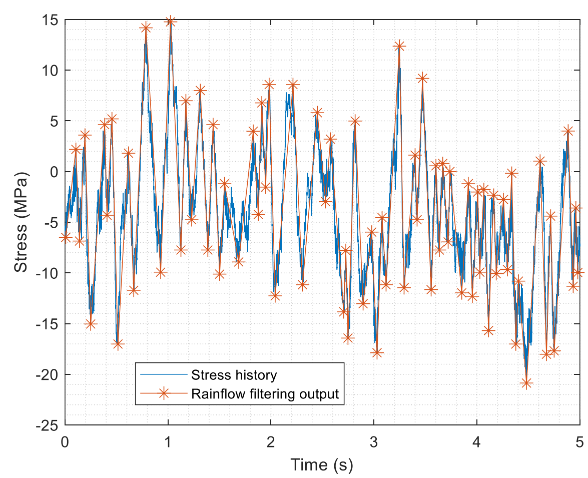

Fig. 4. Turning points outputted by the rainflow counting algorithm.

The rainflow counting output showing the load reversals over time and the distribution of the cycles as a function of the detected stress range and its mean value (rainflow matrix histogram) are shown in Fig. 5. The results of the rainflow counting were then referred to the S-N curve of hard-drawn copper [21] to find the number of cycles to failure at each stress level and to calculate the cumulative damage and the remaining lifetime by using Miner's rule according to (2) and (3), respectively.

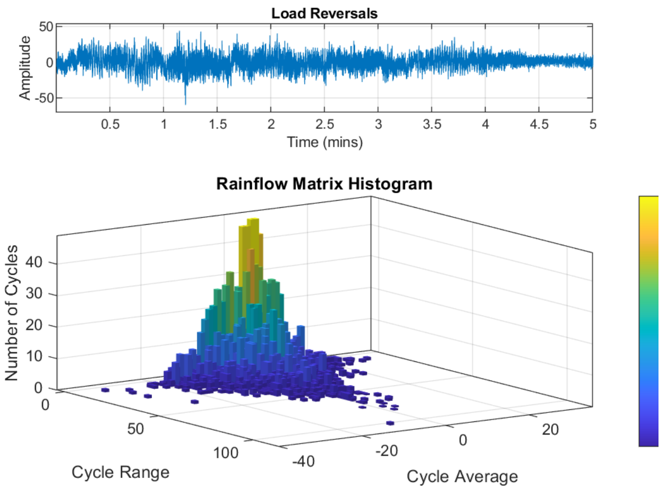

Fig. 5. Load reversals and rainflow matrix histogram.

From the analysis procedure presented above, the cumulative damage was estimated to be equal to $1.1 \cdot 10^{-6}$, indicating that the conductor should not be damaged when subjected to such a stress profile. The estimated lifetime of the conductor was $9.2 \cdot 10^{5}$ cycles.

IV. CONCLUSION

In this paper, methodological framework for estimation of fatigue life of overhead conductor due to aeolian vibration has been implemented using rainflow counting algorithm and miner's rule. The algorithm leverages data from overhead line (OHL) sag and vibration measurements conducted with FBG based sag sensors during a field trial in a simulated power network setting to assess the durability of OHL conductors. The rainflow counting algorithm is helpful for understanding cyclic loading history of overhead line conductors to predict fatigue. It also helps in analyzing stress cycles and assessing structural integrity of conductor with respect to different loads over time. Each applied cycle has different damage factor based on material properties, geometry of conductor and amplitude of load cycle. The cumulative damage estimated at considered stress range is estimated as $1.1 \cdot 10^{-6}$. The result illustrates that the conductor will endure $9.2 \cdot 10^{5}$ cycles of operation.

Future work will focus on experimental fatigue testing of both sensor and conductor to validate the methodology for predicting failure and lifetime of the overhead line conductors.

ACKNOWLEDGMENT

We acknowledge the support of the Engineering and Physical Sciences Research Council and National Physical Laboratory (NPL), contributing to the associated PhD project. All data underpinning this publication are openly available from the University of Strathclyde Knowledge Base at https://doi.org/10.15129/4ed36178-6b24-4a7e-adb3-b1ce6f8cb40c.

REFERENCES

[1] R.B. Kalombo and J.A. Araujo and J.L.A. Ferreira and C.R.M. da Silva and and R. A. and A. R. Capra, "Assessment of the fatigue failure of an All Aluminium Alloy Cable (AAAC) for a 230kV transmission line in the Center-West of Brazil," *Eng. Fail. Anal.*, vol. 61, pp. 77–87, 2016.

[2] C.R.F Azevedo and T Cescon, "Failure analysis of aluminum cable steel reinforced (ACSR) conductor of the transmission line crossing the Parana River," *Eng. Fail. Anal.*, vol. 9, no. 6, pp. 645–664, 2002.

[3] M. Ouaki, B., Goudreau, S., Cardou, A., Fiset, "Fretting fatigue analysis of aluminium conductor wires near the suspension clamp: Metallurgical and fracture mechanics analysis," *J. Strain Anal. Eng. Des.*, vol. 38, no. 2, pp. 133–147, 2003.

[4] M. A. Al Aqil and K. Kopsidas, "Predicting the End-of-Life for OHL Conductors," in *2020 IEEE/PES Transmission and Distribution Conference and Exposition (T&D)*, IEEE, Oct. 2020, pp. 1–5. doi: 10.1109/TD39804.2020.9299663.

[5] K. Kopsidas and S. M. Rowland, "Evaluating opportunities for increasing power capacity of existing overhead line systems," *IET Gener. Transm. \& Distrib.*, vol. 5, no. 1, pp. 1–10, 2011.

[6] IEEE, "Field, IEEE 1368: IEEE Guide for Aeolian Vibration Measurement of Overhead Conductors," 2006. doi: 10.1109/IEEESTD.2006.371267.

[7] IEC Standard 61897, "Overhead Transmission Lines-Requirements and Tests for Stockbridge Type Aeolian Vibration Dampers," 1998.

[8] CIGRE SC22 WG11, "Safe design tension with respect to aeolian vibrations, Part 2: Damped single conductors," 2001.

[9] CIGRE SC B2 WG B2.25, "Assessment of aeolian vibrations severity," 2009.

[10] G. Fusiek and P. Niewczas, "Design of an optical sensor with varied sensitivities for overhead line sag, temperature and vibration monitoring," in *2022 IEEE International Instrumentation and Measurement Technology Conference (I2MTC)*, IEEE, May 2022, pp. 1–6. doi: 10.1109/I2MTC48687.2022.9806489.

[11] G. Fusiek, H. Singh, and P. Niewczas, "Temperature and force characterization of an optical sag sensor for overhead line monitoring ," in *2023 IEEE International Instrumentation and Measurement Technology Conference (I2MTC)*, Apr. 2023.

[12] H. Singh, G. Fusiek, and P. Niewczas, "Extended Characterization of an Optical Sag Sensor for High-Temperature Low-Sag Lines," *IEEE Sensors Lett.*, vol. 7, no. 9, pp. 1–4, Sep. 2023, doi: 10.1109/LSENS.2023.3300810.

[13] H.Singh, G.Fusiek, P.Niewczas and V.Livina, "Estimation of the Fatigue Life of a Fiber Bragg Grating Overhead Line Sag Sensor," in *I2MTC 2024*, 2024, pp. 1–6.

[14] M. Matsuishi and T. Endo, "Fatigue of metals subjected to varying stress," *Japan Soc. Mech. Eng. Fukuoka, Japan*, vol. 68, no. 2, pp. 37–40, 1968.

[15] I. Rychlik, "Fatigue and stochastic loads," *Scand. J. Stat.*, pp. 387–404, 1996.

[16] R. Mendonça, E. Caetano, C. Moutinho, O. A. Saadi, and J. Rodrigues, "Comparison of Fatigue Lifetime Estimation of a Conductor Based on a Standard Vibration Device and Other Structural Health Monitoring System Sensors," 2024, pp. 255–265. doi: 10.1007/978-3-031-47152-0_22.

[17] D. Benasciutti, R. TOVO, and others, "On fatigue damage computation in random loadings with threshold level and mean value influence," *Struct. Durab. Heal. Monit.*, vol. 2, no. 3, pp. 149–164, 2006.

[18] I. Rychlik, "Simulation of load sequences from rainflow matrices: Markov method," *Int. J. Fatigue*, vol. 18, no. 7, pp. 429–438, 1996.

[19] P. JOHANNESSON, "Extrapolation of load histories and spectra," *Fatigue \& Fract. Eng. Mater. \& Struct.*, vol. 29, no. 3, pp. 209–217, 2006, doi: https://doi.org/10.1111/j.1460-2695.2006.00982.x.

[20] C. Concari and G. Bettini, "Embedded implementation of rainflow-counting for on-line predictive maintenance," in *2020 IEEE Energy Conversion Congress and Exposition (ECCE)*, 2020, pp. 981–988.

[21] L. Kunz, "Mechanical properties of copper processed by severe plastic deformation," *Copp. Alloy. Appl. Curr. Performance-Enhancing Process.*, pp. 93–126, 2012.